DFT Modeling of Water-Assisted Hydrogen Peroxide Formation from a C(4a)-(hydro)peroxyflavin

Yılmaz ÖZKILIÇ[1,*]

[1]Department of Chemistry, Faculty of Science and Letters, Istanbul Technical University, Istanbul, Turkey

*Correspondence: ozkilicy@itu.edu.tr

ORCID: https://orcid.org/0000-0001-8524-532X

Abstract: The cofactor of a class A monooxygenase is reduced at an external location of the enzyme and is pulled back into the active site immediately after the reduction. This observation brings the question; is there any defense mechanism of the active site of a monooxygenase against the formation of the harmful hydrogen peroxide from the reactive C(4a)-(hydro)peroxide intermediate? In this study, the barrier energies of, firstly, one to three water molecule mediated uncoupling reaction mechanisms in water exposed reaction conditions were determined. These were found to be facile barriers. Secondly, uncoupling was modeled in the active site of kynurenine 3-monooxygenase complex which was represented with 258 atoms utilizing cluster approach. Comparison of the barrier energy of the cluster model to the models that represent the water exposed conditions revealed that the enzyme does not have an inhibitory reaction site architecture as the compared barrier energies are roughly the same. The main defense mechanism of KMO against the formation of the hydrogen peroxide is deduced to be the insulation, and without this insulation, the monooxygenation would not take place as

the barrier height of the hydrogen peroxide formation within the active site is almost half of that of the monooxygenation.

Key words: Hydrogen peroxide, DFT, mechanism, C(4a)–(hydro)peroxide, uncoupling, kynurenine 3-monooxygenase

1. Introduction

Flavoenzymes are various enzymes such as dehydrogenases, reductases, oxidases and monooxygenases [1–4]. A flavoenzyme's activity strictly depends on an organic cofactor (Figure 1) that is found in two varieties: a flavin mononucleotide (FMN) or a flavin adenine dinucleotide (FAD) [4]. Isoalloxazine ring system of these cofactors is the chemically involved moiety (Figure 1) that takes part in the activation processes, and the remaining part of the molecule holds the cofactor in an interior location of the protein so that the reactions can take place in a buried environment that prevents the disruptive effects of other molecules; especially the solvent water [5].

Oxidases and monooxygenases are responsible for the activation of the molecular oxygen, which in its triplet ground state cannot spontaneously participate in most of the chemical reactions [2]. According to experimental and computational studies, the flavoenzyme catalyzed oxygen activation mechanisms generally involve two half-reactions in which the isoalloxazine ring system is reduced and oxidized consecutively (Figure 1) [6–28]. During the reduction of the class A monooxygenases, FAD changes its conformational state to meet with the large reducing agent NADPH at an outer location of the enzyme then immediately returns to its original conformational state [5]. The details and classifications of these particular reactions are nicely explained in recent reviews [1–3].

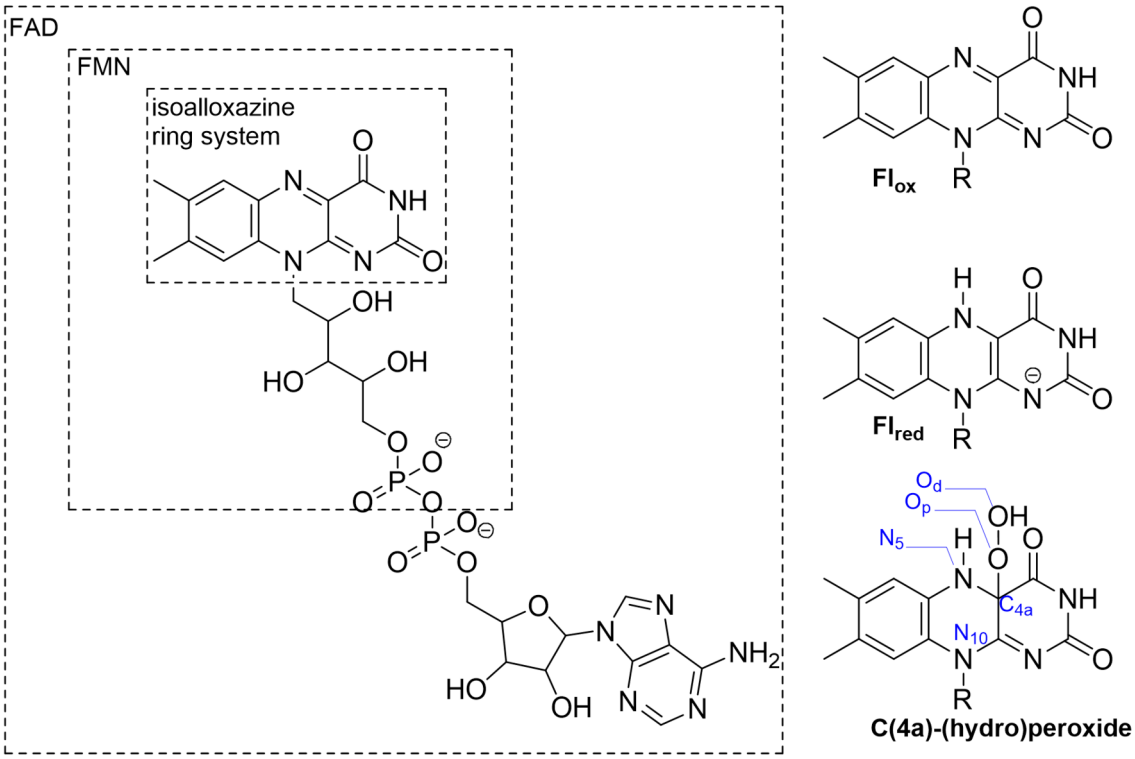

Figure 1. Flavin mononucleotide (FMN) and flavin adenine dinucleotide (FAD) structures with their different oxidation states [2].

The prime objective of the present study is to understand how monooxygenases act like oxidases. In Figure 2, the reactions between reduced flavins and the molecular oxygen are concisely summarized for the oxidases and monooxygenases. Oxidases catalyze the formation of hydrogen peroxide (H_2O_2), while monooxygenases catalyze the formation of an oxygen adduct of a substrate through the reactive C(4a)–(hydro)peroxide intermediate whose one of the oxygen atoms is transferred to the substrate [2]. When this substrate is not present in the active site of a monooxygenase, an event known as uncoupling takes place: hydrogen peroxide is formed through the oxidation of the flavin (Figure 2) [2]. Interestingly, uncoupling can take place even when the substrate is within the active site [29]. Hydrogen peroxide accelerates aging, cancer cell metabolism and inflammation [30]. In addition, hydrogen peroxide increases oxidative stress in

neurons which induces neuronal cell death and thereby can trigger a variety of neurodegenerative diseases [31, 32]. Generation of hydrogen peroxide in a monooxygenase can complicate therapeutic strategies. An infamous example is the inhibition of kynurenine 3-monooxygenase (KMO) whose product's (3-hydroxykynurenine: 3-HK) overproduction is known to cause several neurodegenerative diseases [33, 34]. Most of the KMO inhibitors successfully inhibit the formation of 3-HK and thereby the monooxygenation of the substrate L-kynurenine (L-Kyn), but also can cause the reduction of Fl_{ox} which leads to the formation of the unstable C(4a)–(hydro)peroxide intermediate that inevitably relaxes with uncoupling [29, 35, 36]. Therefore, the struggle to prevent a kind of neurodegenerative disease inducer leads to another due to the complication introduced by the generation of hydrogen peroxide as a side product.

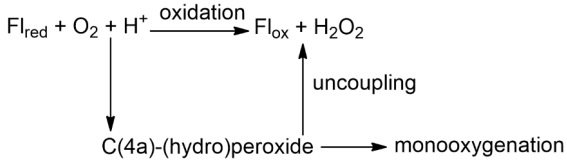

Figure 2. Concise summary of the conventional reactions between reduced flavins (Fl_{red}) and molecular oxygen [11].

According to mechanistic studies, the monooxygenation reaction can take place with lower barrier energies when it is taking place within the active site of a monooxygenase. However, the barrier energy lowering offered by the enzyme is not that significant, meaning that the reaction between the C(4a)–(hydro)peroxide and the substrate would still take place if only the environment's disruptive effect was circumvented [16, 20]. Therefore, the main function of the protein is to provide a selective environment for the relevant substrate and insulate the active site from the solvent water so that the

uncoupling that results in the generation of the harmful hydrogen peroxide can be avoided [16, 20].

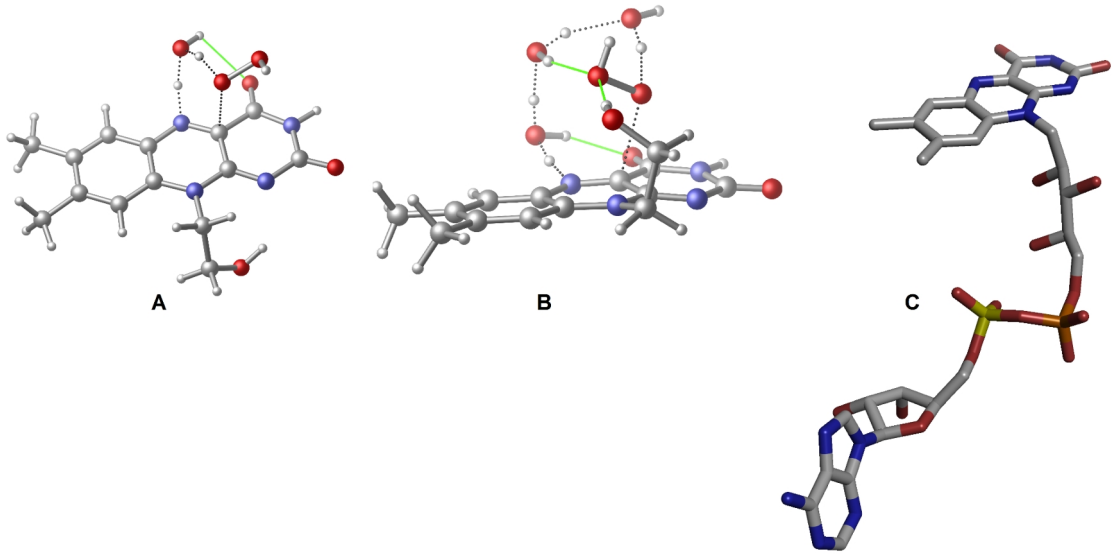

Figure 3. Reference TSs that involve the activation with one water molecule and three water molecules (**A** and **B**, respectively) [25]. The alignment of the isoalloxazine's representative substituent is drastically changed in comparison to its actual alignment (**C**; H atoms are not shown), as seen in a usual monooxygenase (pdb id: 1DOD). The change in **B** is more important because it enables an additional unnatural H-bonding interaction. All the H-bonds are shown in green color.

According to experimental studies, deprotonation of the N_5 atom (for the atomic labels, please see Figure 1) plays a pivotal role in the uncoupling event [37]. Based on these studies, a concerted mechanism was put forward in which the hydrogen of N_5 forms H-bonding interactions with both hydroperoxide oxygen atoms (the one which binds to C_4 carbon is known as the proximal oxygen (O_p) while the other is known as the distal oxygen (O_d), as defined in Figure 1) in the transition state (TS) which is eventually followed by the H_2O_2 release. This idea was challenged by a computational study in

which the authors show how a concerted mechanism would require high barrier energy [25]. Although, according to a more recent calculation the barrier energy of a concerted mechanism was shown to be around 25 kcal/mol for this step, it still cannot compete with monooxygenation [11]. This is important because, as mentioned earlier, the uncoupling in a monooxygenase takes place even in the presence of a substrate. According to the gas phase calculations of the former study, local environment related interactions are necessary for H_2O_2 generation [25]. Naturally, water molecules were one of the investigated effectors of H_2O_2 generation. With the participation of one water molecule as a catalyst, the TS barrier energy required 19.51 kcal/mol, which is a feasible value for a reaction to take place. While the inclusion of a second water molecule did not change the barrier significantly, a TS structure with three water molecules lowered the barrier energy to 16.24 kcal/mol. These calculations certainly should be a step up from the previous proposition since the easy decay of C(4a)-(hydro)peroxide intermediate all by itself would render it useless as a cofactor. These calculations also imply that even a single water molecule can catalyze the decay of the intermediate into its oxidized state (Fl_{ox}) and an H_2O_2 molecule. However, as displayed in some of the X-ray structures, there is a recurring water molecule near the isoalloxazine ring system of a monooxygenase [38, 39]. Moreover, this water molecule was shown to participate in the normal catalytic activity of the enzyme [20]. These calculations should be reconsidered because the remaining part of the flavin, that is bound to the isoalloxazine ring system from the N_{10} position, was modeled as an unrestrained $–(CH_2)_2–OH$ moiety (Figure 3). The hydroxyl of this moiety formed an H-bond with only some of the TS structures, complicating the comparison of TSs with different numbers of water molecules (Figure 3). In its natural environment, this part of

the cofactor can never change its conformation to allow these interactions (Figure 3). Because it corresponds to a large moiety that is buried within the enzyme and stabilized with various residues, which restrict its rotation. In addition, finding the minimum number of water molecules that allow the reaction to evolve with a feasible barrier energy requires reconsideration of these calculations with the right solvation scheme instead of the gas phase.

In this manuscript, firstly, density functional theory (DFT) calculations were carried out to find the minimum number of water molecules necessary to reduce the uncoupling barrier energy to about that of a monooxygenation when the reaction takes place at a water exposed location. Secondly, for the first time in the literature, a quantum-cluster model [40] (please see computational methods for details) of the active site of kynurenine 3-monooxygenase was built to see how the uncoupling reaction takes place within the active site of the enzyme by the activation of water molecules. This study can enhance our understanding of C(4a)-(hydro)peroxyflavin stability which was described as a fundamental challenge in a recent review [2].

2. Computational Methods

The optimizations of the usual models were carried out using Gaussian 16 Revision A.03 software package at the B3LYP/6-31+G(d,p) level of theory [41]. Each TS was confirmed to have only one imaginary frequency. Reactant and product states, which did not have any imaginary frequency apart from the product states **P1v2** (7.85 i s^{-1}) and **P2v2** (12.34 i s^{-1}), were located by following the points obtained from the intrinsic reaction coordinate (IRC) calculations, as implemented in Gaussian 16 [42, 43]. The imaginary frequencies mentioned were ignored because they are very low and belong to the product states that do not affect the forward barrier energies. The solvent water was

represented by polarizable continuum model (PCM) in all of these calculations [44]. In addition, the larger basis set 6-311+G(2d,2p) was utilized in the single point calculations to refine the electronic energies to which DFT-D3(BJ) scheme dispersion corrections [45, 46] and the zero-point energy corrections that were obtained from the optimization level were added while solvent water was represented by PCM.

The active site of KMO was built starting from the X-ray structure 6FOX.pdb for the quantum-cluster modeling that was also previously utilized in the mechanistic studies of KMO [20, 47]. In this model, the FAD unit was mainly modeled as the isoalloxazine ring system. The remaining part of FAD was represented with a methyl moiety whose carbon atom's coordinates were fixed during optimizations. In addition, a hydroperoxide moiety was attached to the C_{4a} position. L-Kyn substrate in the original structure was replaced with a water molecule. The β sheet below the isoalloxazine ring system was represented with the Asn54-Leu55-Ala56-Leu57 array of residues and the positions of the α carbon atoms of Asn54 and Leu57 residues, which were capped with hydrogen atoms, were fixed in their X-ray coordinates. The loop above the isoalloxazine ring system was treated the same way and represented with the Val317-Pro318-Phe319-His320-Gly321-Gln322-Gly323-Met324 array of residues. Ile224, Leu226, Thr236 and Phe238 were represented with their side chains. 8 water molecules that were present in the active site of the X-ray structure were retained in the calculations. The neutral model is comprised of 258 atoms. Nine atoms were fixed in their X-ray positions during the geometry optimizations. The optimizations of the cluster models were carried out at the B3LYP/6-31G(d,p) level of theory. This level of theory proved to be efficient in previous computational studies for this complex [20, 47]. TSs were located as explained above and similarly, the reactant and the product geometries were obtained through the

optimizations of the corresponding IRC point geometries. In the single point calculations, the basis set was enlarged to 6-311+G(2d,2p), and the dispersion and the zero-point energy corrections were added to the electronic energies as described above. These single point calculations were repeated in different dielectric constants (ε=1, 4, 16, 80) to reveal the competency of the size of the cluster models.

3. Results and discussion

Initially, the water-activated uncoupling was studied in a solvent water exposed environment. In this initial study, general conclusions relevant to any monooxygenase are sought. Therefore, the computational system was assumed to be surrounded with water, and the PCM solvation scheme was adapted accordingly to represent the reaction conditions.

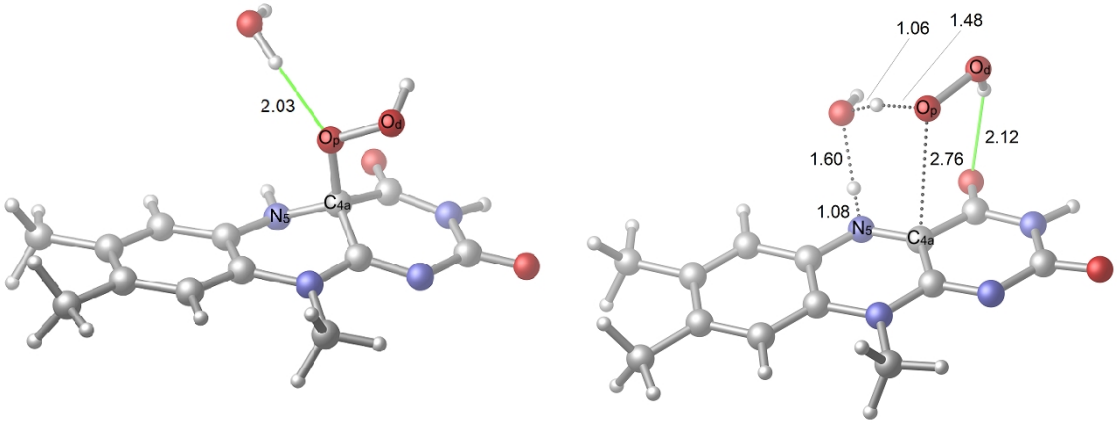

Figure 4. Reactant (**R1v1**) and TS (**TS1v1**) geometries related to the activation with one water molecule. H-bonds are shown in green color.

In the second part of this study, the uncoupling was modeled within the active site of KMO using the quantum-cluster computational scheme. This study can also reveal the importance of the predefined positions of the water molecules observed in the active site of KMO. In a previous computational study [20], it was alluded that there is a conserved

H-bonding network of water molecules in the active site of KMO. This network is observed in different X-ray structures of KMO (5NAK.pdb and 6FOX.pdb) that were obtained by different experimental groups. The current study can reveal new findings about the necessity for these water molecules, which are potential reactants in the uncoupling reaction, to be in predefined positions.

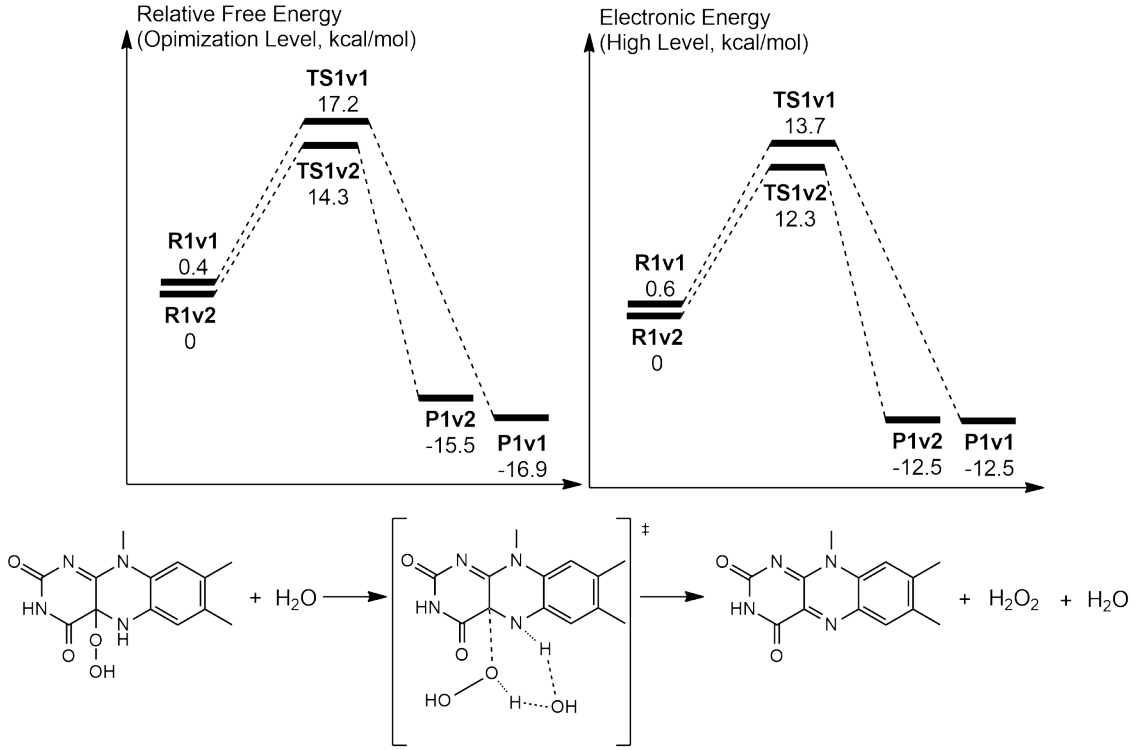

Figure 5. Reaction coordinate related to the activation with one water molecule. Energies are not to scale.

C(4a)-(hydro)peroxide intermediate was modeled as the isoalloxazine ring system that is bound to the hydroperoxy moiety, and the remaining fragment was represented with a methyl moiety. As explained in the introduction, adding the remaining part of this large molecule is unnecessary since it orients further away, and it does not take part in the reaction. Additionally, the inclusion of this part causes problems when the specific enzyme environment is not introduced into the computational system.

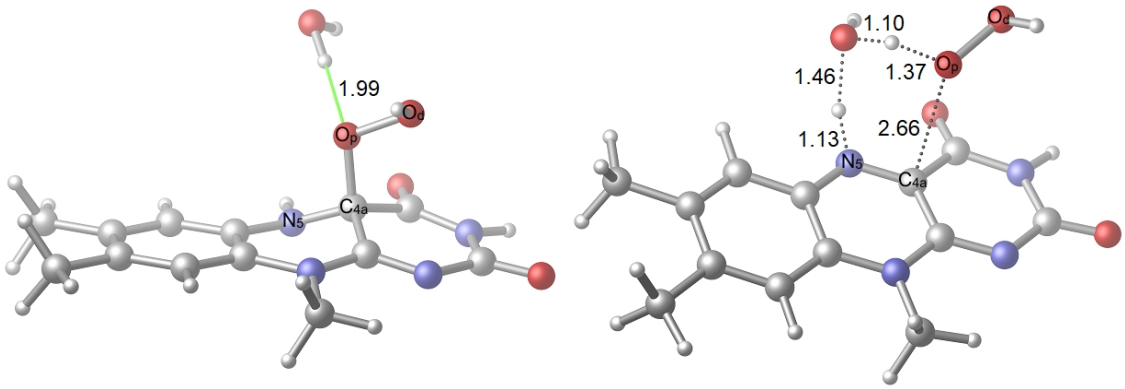

Figure 6. Alternative reactant (**R1v2**) and TS (**TS1v2**) geometries related to the activation with one water molecule. H-bonds are shown in green color.

Herein, we are interested in particular H-bonding possibilities which can activate the uncoupling through a proton shuttle, so N_5 position is considered in the formation of H-bonds, which are mediated by water molecules. The water molecules can interact with other positions of the isoalloxazine ring system, but these are not primary interactions that can aid the activation. Two alternative pathways were considered for the uncoupling mediated by one water molecule. These involve the transfer of the positively charged hydrogen (H^+), which is bound to N_5, to the oxygen atom of a water molecule whose own H^+ is transferred to O_p. This induces the breaking of C_{4a}–O_p bond that liberates a free H_2O_2. In the first case (Figures 4 and 5), the hydroxyl hydrogen of the hydroperoxide moiety orients towards the carbonyl oxygen of the isoalloxazine ring system, where the formation of an H-bonding interaction opportunity arises in the TS structure (**TS1v1**); in the second case (Figures 5 and 6), the hydroxyl hydrogen of the hydroperoxide moiety orients in the opposite direction.

At first glance, it seems that a stabilization possibility was discarded with the second option. However, the first option also involves a repelling interaction due to the proximity of the mentioned hydrogen of hydroperoxide moiety to the H^+ that is being

transferred from the water oxygen to O_p. The comparison of the reactant geometries of the two options in Figures 4 and 6, respectively, shows that they are significantly alike. The only difference is the mentioned orientation of the hydroperoxide hydrogen. This difference in the reactant geometries is not significant thermodynamically since the free energy difference (at the optimization level) between the respective structures is 0.4 kcal/mol while their electronic energy difference (at high-level) is 0.6 kcal/mol. According to the schemes given in Figure 5 there is 2.9 kcal/mol and 1.4 kcal/mol of a reduction in the relative TS free energy and the relative electronic energy from first to the second case, respectively. Therefore, the barrier energy differences are mainly due to the TS energies. These barrier energies (Figure 5) that correspond to the reaction conditions when the hydroperoxide intermediate is vulnerable to the solvent water molecules render the uncoupling reaction feasible.

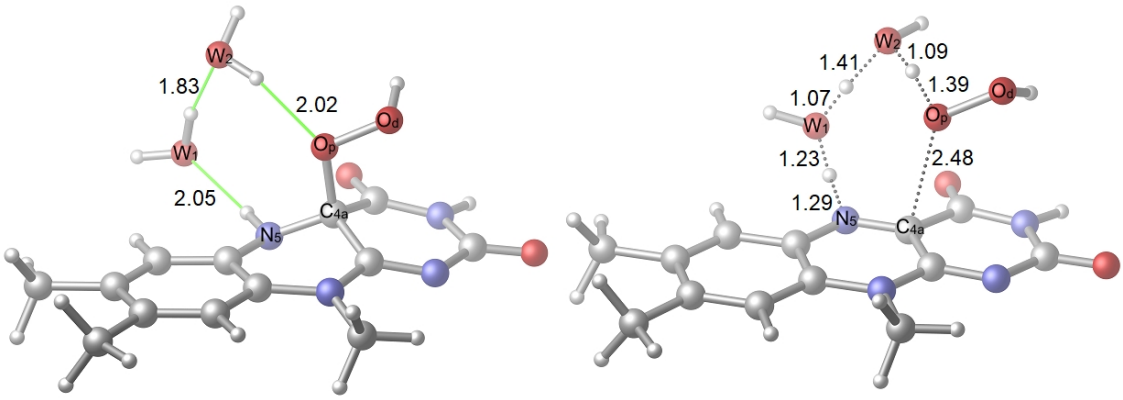

Figure 7. Reactant (**R2v1**) and TS (**TS2v1**) geometries related to the activation with two water molecules. H-bonds are shown in green color.

The reaction was reconsidered with the addition of a second water molecule. Two possibilities that involve the transfer of the H^+ bound to N_5 to the first water (W_1) oxygen whose own H^+ is transferred to the second water (W_2) oxygen were considered. The W_2 was placed between the W_1 and O_p to increase the number of the members of

the proton shuttle so that it can further aid the activation of the uncoupling by decreasing the strain of the TS geometry. Other H-bonding sites were not considered because these sites would not aid the activation as they should do by increasing the size of the proton shuttle. In addition, placing the W_2 in other H-bonding sites would not enable a TS structure similar to what is seen in Figures 7-9 because the W_2 would be further away and can only influence the reaction via a weaker interaction. This proton shuttle induces the transfer of W_2's own H^+ to O_p and the breaking of the C_{4a}–O_p bond that liberates a free H_2O_2.

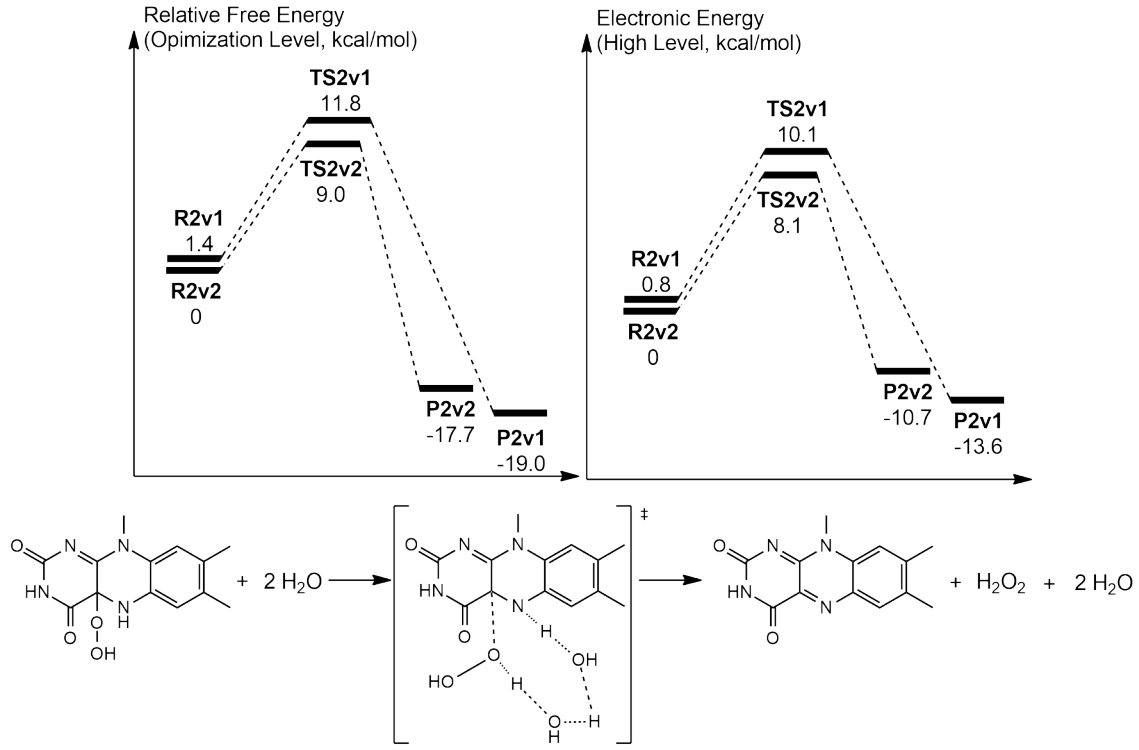

Figure 8. Reaction coordinate related to the activation with two water molecules. Energies are not to scale.

In the first case (Figures 7 and 8), the hydrogen of W_2, whose H^+ is to be transferred to the O_p, can form an H-bonding interaction with the carbonyl oxygen of the isoalloxazine ring system. Here, the orientation of the hydrogen was made available, but the H-bonding interaction was not realized. In the second case (Figures 8 and 9), it is the

hydrogen of W_1 that can form an H-bond with the carbonyl oxygen. Another difference between the two systems is that in the first case, the immobile hydrogen of W_2 points in the same direction as the hydroperoxide hydrogen, while in the second case it points in the opposite direction.

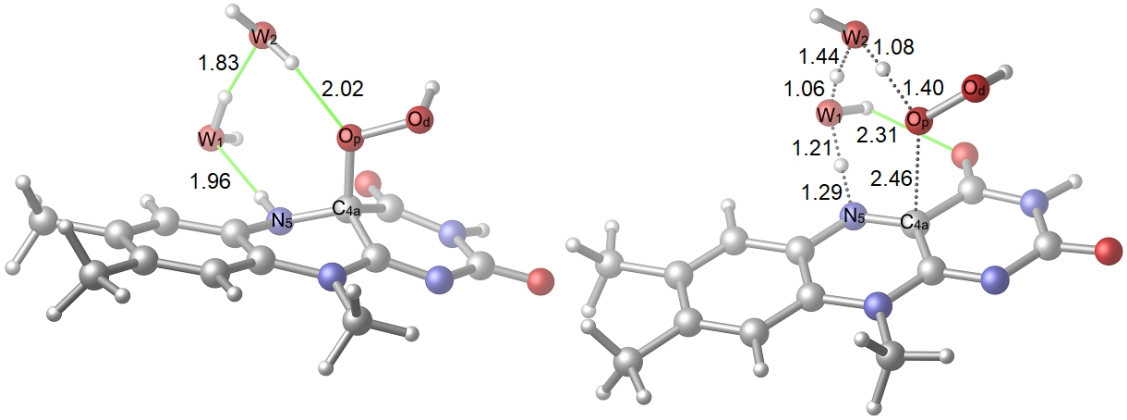

Figure 9. Alternative reactant (**R2v2**) and TS (**TS2v2**) geometries related to the activation with two water molecules. H-bonds are shown in green color.

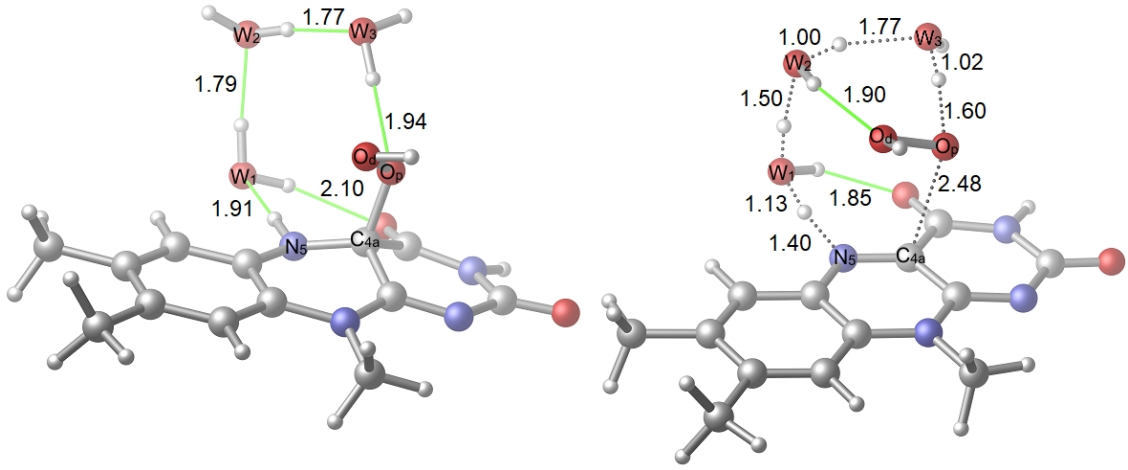

Figure 10. Reactant (**R3**) and TS (**TS3**) geometries related to the activation with three water molecules. H-bonds are shown in green color.

As can be seen in Figure 8, the relative TS free energy of the second case is 2.8 kcal/mol lower in comparison to the first case, while their electronic energy difference

is 2.0 kcal/mol. The difference between the free and the electronic energies of the reactant geometries are 1.4 kcal/mol and 0.8 kcal/mol, respectively. Therefore, in the barrier energy differences (Figure 8) both the reactant and the TS geometries play a significant role.

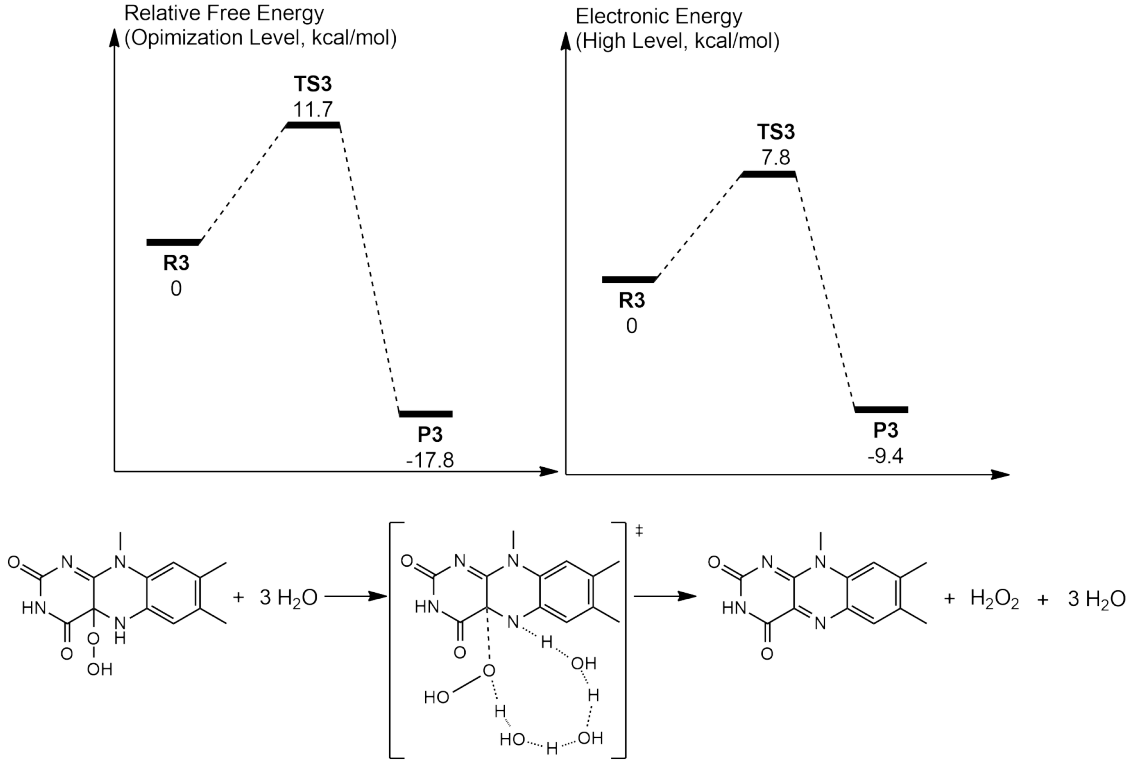

Figure 11. Reaction coordinate related to the activation with three water molecules. Energies are not to scale.

The obtained barrier energy differences can be understood by comparing the reactant and the TS structures given in Figures 7 and 9: In both reactant geometries there is no H-bonding interaction apart from the H-bonding interactions that is going to involve the mobile hydrogen atoms in the corresponding TSs while, as stated, the reactant in the second case is still more stable. However, in the TS structures there is a clear difference: In the first case, there is no H-bonding interaction between the carbonyl oxygen and W_2's hydrogen while in the second case, there is an H-bonding interaction between

W_1's hydrogen and the carbonyl oxygen. Moreover, the repelling interaction between W_2's hydrogen and the hydroperoxide hydrogen is absent in the second case. Therefore, these additional stabilizations render the second case TS – first case TS energy differences more significant in comparison to the second case reactant – first case reactant energy differences. However, both free energy and electronic energy barriers of both reactions activated by two water molecules are lower in comparison to the ones that are activated by one water molecule.

The mechanism of uncoupling with three water molecules (Figures 10 and 11) involves the simultaneous displacement of positively charged hydrogen centers (4 H^+s) from N_5 to O_p direction, through the mediation of three water molecules. This eventually breaks the C_{4a}–O_p bond and liberates a free H_2O_2. The free energy barrier is 11.7 kcal/mol while the electronic energy barrier is 7.8 kcal/mol. Accordingly, the reaction with three water molecules proceeds with a higher free energy barrier while the electronic barrier energy is roughly the same in comparison to the reaction with two water molecules. Therefore, increasing the number of water molecules that mediate the uncoupling reaction is not required, and the reaction activated by two water molecules can be considered the main reaction when the system is exposed to the solvent water.

In the cluster model calculations, just like in a previous computational study [20], the two water oxygen atoms were used to generate the hydroperoxide moiety of the model of C(4a)-(hydro)peroxide intermediate. Their positions allowed modeling this moiety in a way similar to that is seen in the structure **R2v1**. The original positions of these oxygen atoms are suitable to obtain the desired conformational state of the hydroperoxide moiety because the one that corresponds to the proximal oxygen (which is required to interact with the water hydrogen) is closer to the water hydrogen in

comparison to the one that corresponds to the distal oxygen (Figure 12). In this model, the first water molecule (W_1) that is involved in the mediation of the transformation is connected to the H-bonding network that extends with several other water molecules towards the Thr236 hydroxyl (Figure 12). As explained in the methods section, there is one additional water molecule (W_2) that takes the place of the substrate that was present in the original X-ray structure. This new water molecule and the first water molecule that is connected to the H-bonding network were used as the mediating agents in the formation of the TS.

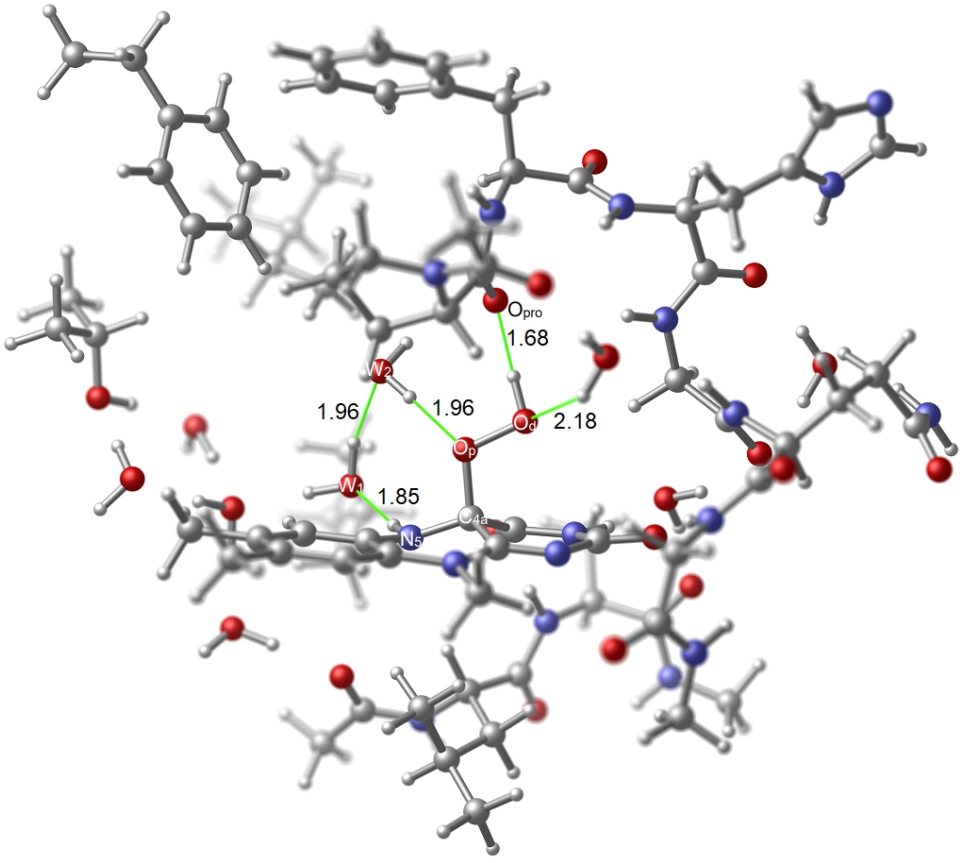

Figure 12. Reactant (**RC**) geometry related to the activation within the active site of KMO. Few important H-bonds are shown in green color. Several atoms were left out of focus to make the involved portion of the model apparent.

The active site of the KMO is extremely restrictive. For example, it does not allow a TS model as seen in **TS2v2** because if the orientation of the immobile hydrogen of the second water molecule is as in the **TS2v2**, it causes steric clashes with the hydrogen atoms that are attached to the ring of Pro318. In addition, the removal of L-Kyn from the active site was strictly necessary as it blocks the formation of the H-bonding network that is seen in **R1v1** or **R2v1**. Therefore, the sealing effect of the substrate that was previously alluded is once again reinforced in this study. This means that if the substrate is within the active site of the enzyme while the uncoupling reaction is taking place, its position must be altered in a way that it should not block the formation of an H-bonding interaction like the one seen in **R2v1**. A TS structure that was mediated by three water molecules is not necessary as described above, since this results in a higher barrier. Even if it were not the case, the formation of a TS structure like **TS3** would not be possible as the residues in the loop above the isoalloxazine ring system clash with the mobile atoms of such TS.

As can be seen in Figure 12, one water molecule that originates from the X-ray structure stabilizes the distal oxygen atom with an H-bonding interaction while the hydrogen that is bound to the distal oxygen atom is stabilized by the H-bonding interaction that it forms with the oxygen atom of Pro318's carbonyl (O_{pro}). Stabilization with the O_{pro} is a conserved trait in the monooxygenation reaction [20]. Therefore, adopting a TS geometry that benefits from this interaction is suitable in the uncoupling reaction as well.

As can be seen in Figure 13, in the TS structure, many distances are roughly retained in comparison to those in the model TS (**TS2v1** in Figure 7). The most apparent variation in the distances is seen in the C_{4a}–O_p separation which is shortened by 0.33 Å in

comparison to that in **TS2v1**. This contraction is compensated with the increase in the reaction path distances (dotted lines) between the W_1 oxygen and the W_2 oxygen (0.12 Å), and the W_2 oxygen and the proximal oxygen (0.14 Å). There is no variation in the reaction path distance between the N_5 and the W_1 oxygen. The stabilizations obtained by the H-bonding interactions between the hydroperoxide moiety and the O_{pro} or the nearby water hydrogen are retained to a great extent in comparison to those in the reactant structure (**RC**), since the O_{pro} – hydroperoxide hydrogen, and the O_d – the water hydrogen distances vary slightly, 0.12 Å and -0.26 Å, respectively, and in reverse directions.

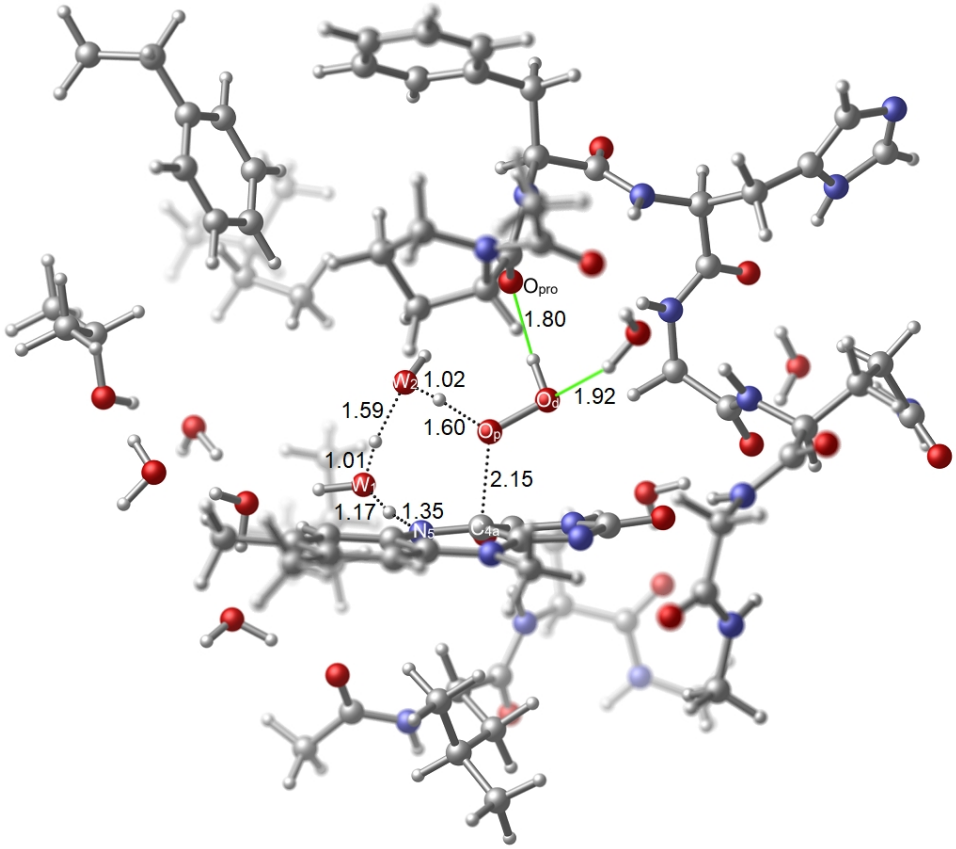

Figure 13. TS (**TSC**) geometry related to the activation within the active site of KMO. Few important H-bonds are shown in green color. Several atoms were left out of focus to make the involved portion of the model apparent.

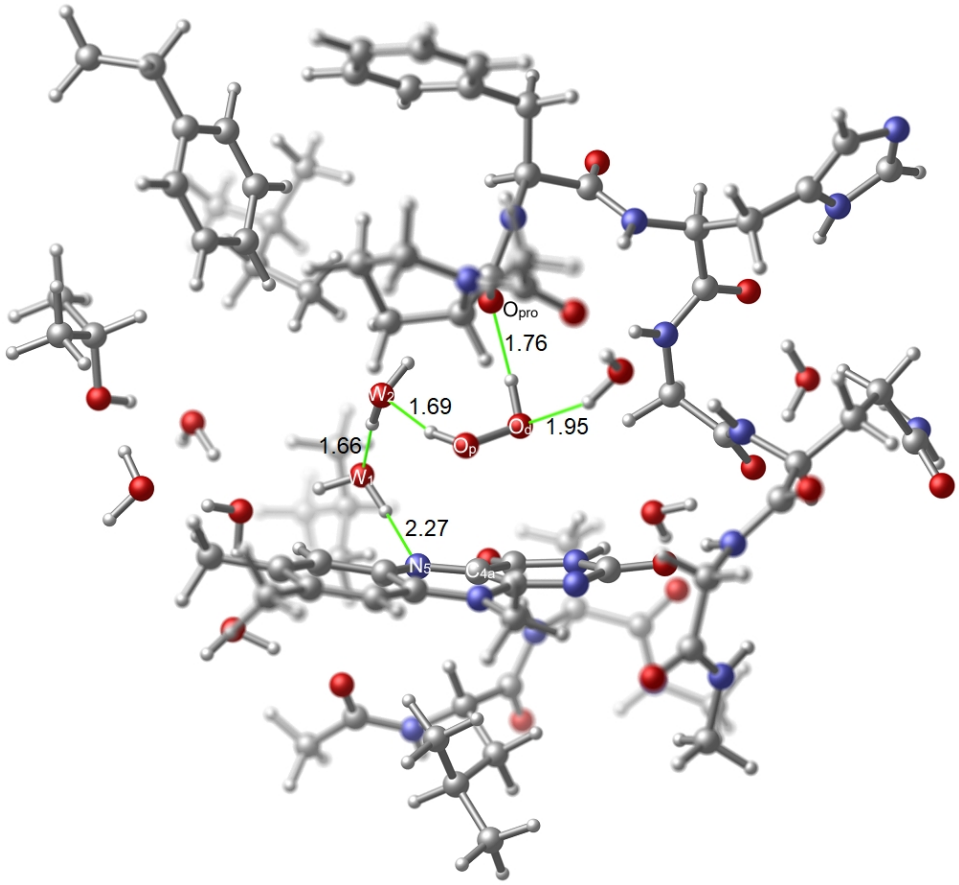

Figure 14. Product (**PC**) geometry related to the activation within the active site of KMO. Few important H-bonds are shown in green color. Several atoms were left out of focus to make the involved portion of the model apparent.

The conservation of the mentioned geometrical features in **TSC** in comparison to both **TS2v1** and **RC** is reflected in the thermochemistry of the reaction as can be seen by comparing the energies presented in Figures 8 and 15. The free energy barrier of the cluster model changes 0.3 kcal/mol while the electronic energy barrier changes -0.7 kcal/mol in comparison to the corresponding barriers seen in Figure 8 for the first case. Here, we stated the electronic energies when ε=4.0 but as it will become clear in the following discussion, the variation of the dielectric constant does not affect the reaction thermochemistry, which reveals the competency of the size of the cluster model.

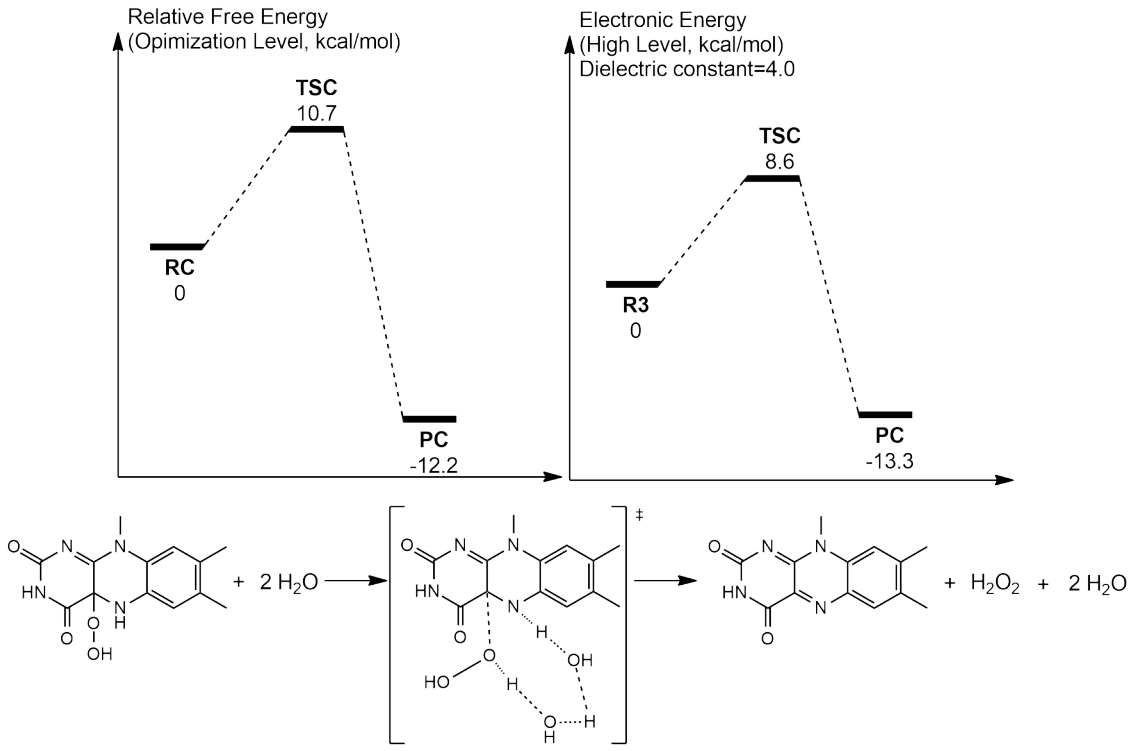

Figure 15. Reaction coordinate related to uncoupling within the active site of KMO. Energies are not to scale.

Formation of the H_2O_2 is completed in the product state of the cluster model (**PC** in Figure 14) where H_2O_2 is stabilized through several H-bonding interactions within the active site and the model FAD returns to its original oxidation state.

The comparison of the high-level electronic energy barrier (with said corrections at ε=4.0) of the uncoupling to that of the monooxygenation of L-Kyn allows the revelation about the reaction site inhibitory capability against the uncoupling reaction. According to previous two computational studies in which the same cluster approach scheme was utilized, the high-level electronic energy barrier (with said corrections at ε=4.0) of the monooxygenation was found as 19.7 kcal/mol or 16.2 kcal/mol depending on the conformational state of the starting X-ray structure [20, 47]. These values are clearly higher than the one (8.6 kcal/mol in Figure 15) found for the uncoupling reaction in this study. According to these values, if the overall enzyme architecture every once in a

while allows the permeation of water molecules into the reaction site with a configuration as described for the cluster models, the uncoupling that has a lower barrier height can take place, instead of the monooxygenation of L-Kyn. The active site has the ability to block the water molecules most of the time, since the production of 3-HK by the monooxygenation of L-Kyn is an experimentally established fact. Another condition for the uncoupling to take place within the active site is the movement of L-Kyn away from the reaction site. Insulation is the main defense mechanism of KMO against the decay of C(4a)-(hydro)peroxide by uncoupling since the reaction site architecture allows uncoupling. This insulation also includes the water molecules being at the predefined positions within the active site, and the blocking effect of the L-Kyn.

The reduction of FAD's isoalloxazine ring system by NADPH was hypothesized to take place at an exterior location but the corresponding short-lived conformational state has never been observed [29]. According to this hypothesis, after the reduction takes place, the conformational state of FAD changes instantly and the reduced isoalloxazine ring system returns to its original location in the active site. Although uncoupling at an exterior location is energetically feasible all by itself, the fact that it depends on an unstable conformational state must be noted. Uncoupling at an external location also requires the rapid oxygenation [35] to take place therein so that the reactive hydroperoxide intermediate can form.

According to Table 1, the change of the dielectric constant does not strongly influence the relative energy differences. The most apparent deviation was seen in the barrier energy of the ε=1.0 solvation scheme. The other values are almost equivalent. Even the barrier energy of the ε=1.0 solvation scheme deviates only about 1 kcal/mol relative to

the barrier energies of other solvation schemes. These results clearly validate the competency of the size of the computational system.

Table 1. High-level electronic energies (kcal/mol) with respect to different dielectric constants. The energies are calculated relative to the reactant state (**RC**) in each solvation scheme.

State	$\epsilon = 1$	$\epsilon = 4$	$\epsilon = 16$	$\epsilon = 80$
RC	0	0	0	0
TSC	9.6	8.6	8.6	8.8
PC	-12.9	-13.3	-13.3	-13.6

4. Conclusion

In this manuscript, the formation of free hydrogen peroxide due to the decay of the reactive C(4a)–(hydro)peroxide via uncoupling was investigated. The reaction was considered in two different environments: Firstly, when the reaction system is exposed to solvent water; and secondly, when the reaction system is isolated from the solvent water within the active site of an enzyme, KMO. According to the results of the first part, the reaction is mediated by two water molecules in the working mechanism, since the reaction activated by one water molecule results in higher barrier energies while the reaction activated by three water molecules results in higher free energy barrier and roughly the same high-level electronic energy barrier. Nonetheless, all three mechanistic pathways are feasible and therefore, when the reaction system is exposed to solvent water every one of them can take place to some extent. According to the second part of this study in which the quantum cluster approach was utilized in modeling the uncoupling reaction within the active site of KMO complex that was represented with 258 atoms, the reaction site of KMO does not inhibit the uncoupling because the barrier energies were found to be very similar to that of the model with two water molecules

that is exposed to solvent water. Therefore, the reaction is feasible. The barrier energy of the uncoupling being almost half of that of the monooxygenation of L-Kyn renders it inevitable once a water molecule enters into the active site and the substrate L-Kyn (which blocks the formation of any kind of uncoupling TS that is studied in this manuscript) is moved away. These results imply that the observed hydrogen peroxide formation by uncoupling is either due to the permeation of water molecules into the reaction site or formation of the hydroperoxide intermediate at an external location of the enzyme. However, it must be noted that the duration of the conformational state of FAD that allows it to be at an external location must be extremely short, since this conformational state has never been observed [35].

These results strengthen the thesis that the main defense mechanism of a monooxygenase is insulation. The insulation of KMO also includes the blocking of the water molecules by the substrate L-Kyn itself which seals the entrance to the reaction site as seen in the X-ray structures. The presence of the water molecules at predefined positions [20], as seen within the active sites of different KMO–L-Kyn X-ray structures, must be due to the insulation mechanism because these water molecules are potential catalysts in the uncoupling reaction.

Acknowledgment

The numerical calculations reported in this paper were performed at TUBITAK ULAKBIM, High Performance and Grid Computing Center (TRUBA resources).

References

[1] Toplak M, Matthews A, Teufel R. The devil is in the details: The chemical basis and mechanistic versatility of flavoprotein monooxygenases. Archives of Biochemistry and Biophysics 2021; 698: 108732. \\doi: 10.1016/j.abb.2020.108732

[2] Romero E, Gómez Castellanos JR, Gadda G, Fraaije MW, Mattevi A. Same Substrate, Many Reactions: Oxygen Activation in Flavoenzymes. Chemical Reviews 2018; 118(4): 1742–69. doi: 10.1021/acs.chemrev.7b00650

[3] Cibulka R, Fraaije MW. Flavin-Based Catalysis. Weinheim, Germany: Wiley-VCH, 2021.

[4] Joosten V, van Berkel WJ. Flavoenzymes. Current Opinion in Chemical Biology 2007; 11(2): 195-202. doi: 10.1016/j.cbpa.2007.01.010

[5] Gatti DL, Palfey BA, Lah MS, Entsch B, Massey V et al. The Mobile Flavin of 4-OH Benzoate Hydroxylase. Science (80-) 1994; 266(5182): 110–4. doi: 10.1126/science.7939628

[6] Sucharitakul J, Chaiyen P, Entsch B, Ballou DP. Kinetic mechanisms of the oxygenase from a two-component enzyme, p-hydroxyphenylacetate 3-hydroxylase from Acinetobacter baumannii. Journal of Biological Chemistry 2006; 281(25) :17044–53. doi: 10.1074/jbc.M512385200

[7] Teufel R, Stull F, Meehan MJ, Michaudel Q, Dorrestein PC et al. Biochemical establishment and characterization of EncM's flavin-N5-oxide cofactor. Journal of the American Chemical Society 2015; 137(25): 8078–85. doi: 10.1021/jacs.5b03983

[8] Kiess M, Hecht H, Kalisz HM. Glucose oxidase from Penicillium amagasakiense: Primary structure and comparison with other glucose-methanol-choline (GMC) oxidoreductases. European Journal of Biochemistry 1998; 252(1): 90–9. doi: 10.1046/j.1432-1327.1998.2520090.x

[9] Sanner C, Macheroux P, Rüterjans H, Müller F, BACHER A. 15N-and 13C-NMR investigations of glucose oxidase from Aspergillus niger. European Journal of Biochemistry 1991; 196(3): 663–72. doi: 10.1111/j.1432-1033.1991.tb15863.x

[10] Klinman JP. How do enzymes activate oxygen without inactivating themselves? Accounts of Chemical Research 2007; 40(5): 325–33. doi: 10.1021/ar6000507

[11] Wongnate T, Surawatanawong P, Visitsatthawong S, Sucharitakul J, Scrutton NS, Chaiyen P. Proton-Coupled Electron Transfer and Adduct Configuration Are Important for C4a-Hydroperoxyflavin Formation and Stabilization in a Flavoenzyme. Journal of the American Chemical Society 2014; 136(1): 241–53. doi: 10.1021/ja4088055

[12] Entsch B, Ballou DP, Massey V. Flavin-oxygen derivatives involved in hydroxylation by p-hydroxybenzoate hydroxylase. Journal of Biological Chemistry 1976; 251(9): 2550–63. doi: 10.1016/S0021-9258(17)33523-8

[13] Chakraborty S, Ortiz-Maldonado M, Entsch B, Ballou DP. Studies on the mechanism of p-hydroxyphenylacetate 3-hydroxylase from Pseudomonas aeruginosa: a system composed of a small flavin reductase and a large flavin-dependent oxygenase. Biochemistry 2010; 49(2): 372–85. doi:10.1021/bi901454u

[14] Polyak I, Reetz MT, Thiel W. Quantum Mechanical/Molecular Mechanical Study on the Mechanism of the Enzymatic Baeyer–Villiger Reaction. Journal of the American Chemical Society 2012; 134(5): 2732–41. doi: 10.1021/ja2103839

[15] Wang X-L, Quan J-M. Intermediate-Assisted Multifunctional Catalysis in the Conversion of Flavin to 5,6-Dimethylbenzimidazole by BluB: A Density Functional

Theory Study. Journal of the American Chemical Society 2011; 133(11): 4079–91. doi: 10.1021/ja1106207

[16] Ridder L, Harvey JN, Rietjens IMCM, Vervoort J, Mulholland AJ. Ab initio QM/MM modeling of the hydroxylation step in p-hydroxybenzoate hydroxylase. The Journal of Physical Chemistry B 2003; 107(9): 2118–26. doi: 10.1021/jp026213n

[17] Bach RD. Role of the somersault rearrangement in the oxidation step for flavin monooxygenases (FMO). A comparison between FMO and conventional xenobiotic oxidation with hydroperoxides. The Journal of Physical Chemistry A 2011; 115(40): 11087–100. doi: 10.1021/jp208087u

[18] Sheng D, Ballou DP, Massey V. Mechanistic Studies of Cyclohexanone Monooxygenase: Chemical Properties of Intermediates Involved in Catalysis. Biochemistry 2001; 40(37): 11156–67. doi:10.1021/bi011153h

[19] Bach RD, Dmitrenko O. Electronic requirements for oxygen atom transfer from alkyl hydroperoxides. Model studies on multisubstrate flavin-containing monooxygenases. The Journal of Physical Chemistry B 2003; 107(46): 12851–61. doi: 10.1021/jp035289w

[20] Özkılıç Y, Tüzün NŞ. Computational Survey of Recent Experimental Developments in the Hydroxylation Mechanism of Kynurenine 3-Monooxygenase. The Journal of Physical Chemistry A 2021; 125(43): 9459–77. doi: 10.1021/acs.jpca.1c05397

[21] Mata RA, Werner H-J, Thiel S, Thiel W. Toward accurate barriers for enzymatic reactions: QM/MM case study on p-hydroxybenzoate hydroxylase. The Journal of Chemical Physics 2008; 128(2): 01B610. Doi: 10.1063/1.2823055

[22] Sucharitakul J, Tongsook C, Pakotiprapha D, van Berkel WJH, Chaiyen P. The reaction kinetics of 3- hydroxybenzoate 6-hydroxylase from Rhodococcus jostii RHA1 provide an understanding of the para-hydroxylation enzyme catalytic cycle. Journal of Biological Chemistry 2013 6; 288(49): 35210–21. doi: 10.1074/jbc.M113.515205

[23] Visitsatthawong S, Chenprakhon P, Chaiyen P, Surawatanawong P. Mechanism of oxygen activation in a flavin-dependent monooxygenase: a nearly barrierless formation of C4a-hydroperoxyflavin via proton-coupled electron transfer. Journal of the American Chemical Society 2015; 137(29): 9363–74. doi: 10.1021/jacs.5b04328

[24] Ortiz-Maldonado M, Entsch B, Ballou DP. Oxygen Reactions in p-Hydroxybenzoate Hydroxylase Utilize the H-Bond Network during Catalysis. Biochemistry 2004; 43(48): 15246–57. doi:10.1021/bi048115t

[25] Bach RD, Mattevi A. Mechanistic Aspects Regarding the Elimination of H2O2 from C(4a)-Hydroperoxyflavin. The Role of a Proton Shuttle Required for H2O2 Elimination. The Journal of Organic Chemistry 2013; 78(17): 8585–93. doi: 10.1021/jo401274u

[26] Roth JP, Klinman JP. Catalysis of electron transfer during activation of O2 by the flavoprotein glucose oxidase. Proceedings of the National Academy of Sciences 2003; 100(1): 62–7. doi: 10.1073/pnas.252644599

[27] Su Q, Klinman JP. Nature of Oxygen Activation in Glucose Oxidase from Aspergillus niger: The Importance of Electrostatic Stabilization in Superoxide Formation. Biochemistry 1999; 38(26): 8572–81. doi: 10.1021/bi990044o

[28] Wagner MA, Jorns MS. Monomeric Sarcosine Oxidase: 2. Kinetic Studies with Sarcosine, Alternate Substrates, and a Substrate Analogue. Biochemistry 2000; 39(30): 8825–9. doi: 10.1021/bi000350y

[29] Kim HT, Na BK, Chung J, Kim S, Kwon SK et al. Structural Basis for Inhibitor-Induced Hydrogen Peroxide Production by Kynurenine 3-Monooxygenase. Cell Chemical Biology 2018; 25(4): 426-438.e4. \\doi: 10.1016/j.chembiol.2018.01.008

[30] Lisanti MP, Martinez-Outschoorn UE, Lin Z, Pavlides S, Whitaker-Menezes D et al. Hydrogen peroxide fuels aging, inflammation, cancer metabolism and metastasis: the seed and soil also needs "fertilizer". Cell Cycle. 2011; 10(15): 2440–9. doi: 10.4161/cc.10.15.16870

[31] Nakamura J, Purvis ER, Swenberg JA. Micromolar concentrations of hydrogen peroxide induce oxidative DNA lesions more efficiently than millimolar concentrations in mammalian cells. Nucleic Acids Research 2003; 31(6): 1790–5. doi: 10.1093/nar/gkg263

[32] Whittemore ER, Loo DT, Watt JA, Cotmans CW. A detailed analysis of hydrogen peroxide-induced cell death in primary neuronal culture. Neuroscience 1995; 67(4): 921–32. doi: 10.1016/0306-4522(95)00108-U

[33] Guidetti P, Bates GP, Graham RK, Hayden MR, Leavitt BR et al. Elevated brain 3-hydroxykynurenine and quinolinate levels in Huntington disease mice. Neurobiology of Disease 2006; 23(1): 190–7. doi: 10.1016/j.nbd.2006.02.011

[34] Guidetti P, Luthi-Carter RE, Augood SJ, Schwarcz R. Neostriatal and cortical quinolinate levels are increased in early grade Huntington's disease. Neurobiology of Disease 2004; 17(3): 455–61. doi: 10.1016/j.nbd.2004.07.006

[35] Crozier-Reabe KR, Phillips RS, Moran GR. Kynurenine 3-Monooxygenase from Pseudomonas fluorescens: \\Substrate-like Inhibitors both Stimulate Flavin Reduction and Stabilize the Flavin-Peroxo Intermediate yet Result in the Production of Hydrogen Peroxide. Biochemistry 2008; 47(47): 12420-33. doi: 10.1021/bi8010434

[36] Phillips RS, Iradukunda EC, Hughes T, Bowen JP. Modulation of Enzyme Activity in the Kynurenine Pathway by Kynurenine Monooxygenase Inhibition. Frontiers in Molecular Biosciences 2019; 6: 3. doi: 10.3389/fmolb.2019.00003

[37] Sucharitakul J, Wongnate T, Chaiyen P. Hydrogen peroxide elimination from C4a-hydroperoxyflavin in a flavoprotein oxidase occurs through a single proton transfer from flavin N5 to a peroxide leaving group. Journal of Biological Chemistry 2011; 286(19): 16900–9. doi: 10.1074/jbc.M111.222976

[38] Zhang S, Sakuma M, Deora GS, Levy CW, Klausing A et al. A brain-permeable inhibitor of the neurodegenerative disease target kynurenine 3-monooxygenase prevents accumulation of neurotoxic metabolites. Communications Biology 2019; 2(1): 1–10. doi: 10.1038/s42003-019-0520-5

[39] Hutchinson JP, Rowland P, Taylor MRD, Christodoulou EM, Haslam C et al. Structural and mechanistic basis of differentiated inhibitors of the acute pancreatitis target kynurenine-3-monooxygenase. Nature Communications 2017; 8: 1–12. doi: 10.1038/ncomms15827

[40] Sheng X, Himo F. The Quantum Chemical Cluster Approach in Biocatalysis. Accounts of Chemical Research. 2023; 56(8):v938-47. doi: 10.1021/acs.accounts.2c00795

[41] Frisch MJ, Trucks GW, Schlegel HB, Scuseria GE, Robb MA et al. Gaussian 16, Revision A.03. Wallingford CT: Gaussian, Inc.; 2016.

[42] Hratchian HP, Schlegel HB. Accurate reaction paths using a Hessian based predictor–corrector integrator. The Journal of chemical physics 2004; 120(21): 9918–24. doi: 10.1063/1.1724823

[43] Hratchian HP, Schlegel HB. Using Hessian updating to increase the efficiency of a Hessian based predictor-corrector reaction path following method. Journal of Chemical Theory and Computation 2005; 1(1): 61–9. doi: 10.1021/ct0499783

[44] Tomasi J, Mennucci B, Cammi R. Quantum mechanical continuum solvation models. Chemical Reviews 2005; 105(8): 2999–3094. doi: 10.1021/cr9904009

[45] Grimme S, Antony J, Ehrlich S, Krieg H. A consistent and accurate ab initio parametrization of density functional dispersion correction (DFT-D) for the 94 elements H-Pu. The Journal of Chemical Physics 2010; 132(15): 154104. doi: 10.1063/1.3382344

[46] Grimme S, Ehrlich S, Goerigk L. Effect of the damping function in dispersion corrected density functional theory. Journal of Computational Chemistry 2011; 32(7): 1456–1465. doi: 10.1002/jcc.21759

[47] Özkılıç Y, Tüzün NŞ. Mechanism of kynurenine 3-monooxygenase-catalyzed hydroxylation reaction: a quantum cluster approach. The Journal of Physical Chemistry A 2019; 123(14): 3149-59. doi: 10.1021/acs.jpca.8b11831